Downloaded from rsta.royalsocietypublishing.org

PHILOSOPHICAL TRANSACTIONS OF THE ROYAL SOCIETY A MATHEMATICAL, PHYSICAL & ENGINEERING SCIENCES

Electron scattering by surface adsorbates

The Royal Society

Phil. Trans. R. Soc. Lond. A 1999 **357**, 1143-1160
doi: 10.1098/rsta.1999.0368

Email alerting service

Receive free email alerts when new articles cite this article - sign up in the box at the top right-hand corner of the article or click **here**

To subscribe to *Phil. Trans. R. Soc. Lond. A* go to: **http://rsta.royalsocietypublishing.org/subscriptions**

This journal is © 1999 The Royal Society

Downloaded from rsta.royalsocietypublishing.org

THE ROYAL SOCIETY

Electron scattering by surface adsorbates

By P. G. Burke[1], K. Higgins[1] and J. E. Inglesfield[2]

[1]*Department of Applied Mathematics and Theoretical Physics, The Queen's University of Belfast, Belfast BT7 1NN, UK*
[2]*Department of Physics and Astronomy, University of Wales, Cardiff, PO Box 913, Cardiff CF2 3YB, UK*

Theoretical and experimental methods used to describe electron scattering by surface adsorbates are reviewed. A new R-matrix theory, which describes electron scattering by diatomic molecules physisorbed on a surface modelled by a jellium potential, is then described. This theory provides an accurate description of the molecular wave function and enables the scattered part of the wave function, excluding the incident wave, to be calculated directly. Preliminary calculations for nitrogen orientated perpendicular to a metallic jellium surface are then presented and future directions of research are discussed.

Keywords: R-matrix theory; surface adsorbates; physisorbed molecule; LEED; electron scattering; nitrogen molecule

1. Introduction

Electron scattering by molecules in the gas phase has led to a deep understanding of electronic structure as well as having provided detailed information on excitation, ionization and dissociation processes of importance in many applications. In a similar way, the process of electron scattering by surface adsorbates provides a valuable tool in the determination of both surface and adsorbate structure, as well as giving information on the orientation, excitation, ionization and dissociation of the adsorbate molecules. Both elastic and inelastic scattering experiments have been carried out in this work, using, respectively, low-energy electron diffraction (LEED) and high-resolution electron energy loss spectroscopy (HREELS) techniques, where the types of interaction between a molecule and a surface are conventionally divided into two categories, physisorption and chemisorption, according to the strength of the bonding between the surface and the substrate. In this article we confine our discussion to physisorbed molecules, where the bonding is relatively weak with the result that the properties of the molecule, such as electronic structure and vibrational frequencies, are changed only slightly from those of the free molecule.

The theoretical investigation of scattering by adsorbates has also intensified in recent years with particular emphasis on the effects of resonance states (Palmer & Rous 1992). This is due to their importance in a number of electron spectroscopies, as well as their role in a wide range of dynamical processes at surfaces, such as photodesorption, molecule–surface scattering and dissociative molecular adsorption. However, one of the main drawbacks of previous theories and calculations describing electron scattering by surface adsorbates is the inadequate description of the target molecular wave function (Guyacq *et al*. 1997). The theory presented in this paper represents an improvement on this earlier work in that we have adopted an accurate

© 1999 The Royal Society
TEX Paper

Downloaded from rsta.royalsocietypublishing.org

configuration interaction description of the target molecule in the presence of the surface potential, and we have used an *ab initio* R-matrix description of the electron scattering process. In addition we have developed a formalism in which we calculate the scattering part of the wave function directly excluding the incident wave. This has some analogies to the approach adopted by other workers (Aers *et al*. 1981), who drew on photoemission and LEED theory to study HREELS. Consequently, we are able to circumvent the convergence problems that arise with methods that require the calculation of the total wave function.

In §§ 2 and 3, we describe both the experimental and theoretical methods which have been applied most successfully to this scattering problem, before explaining our new R-matrix approach in § 4. We conclude by discussing the calculation currently underway and showing some preliminary results.

2. Adsorbate scattering in low-energy electron diffraction

Low-energy electron diffraction (LEED), using electrons with an energy of typically 50–300 eV, is one of the most important techniques for determining the structure of surfaces; both clean surfaces and surfaces with adsorbates (Pendry 1994; Van Hove & Somorjai 1994; Van Hove *et al*. 1986). The advantage of scattering electrons in this energy range is the inherent surface sensistivity, due to the short mean free path inside the solid, typically *ca.* 5 Å (Duke 1994), so that the elastically scattered electrons have only penetrated a few atomic layers into the solid. The disadvantage of LEED is that the elastic scattering is strong, hence multiple scattering is important (Pendry 1994). This is quite different from X-ray diffraction, where the scattering by each atom is weak, and the total scattering factorizes into a structure factor and atomic form factors. To interpret LEED spectra, which show the electron current in each diffraction beam as a function of electron energy, computed spectra based on hypothetical structures are compared with experiment. However, very efficient computational techniques for LEED analysis have now been developed, and hundreds of structures have been determined, with a precision that can be better than a few hundredths of an angstrom (Rous 1995*b*).

We begin by considering the elastic scattering of electrons by an ideal surface, i.e. a surface with perfect, two-dimensional periodicity (Van Hove *et al*. 1986). The incident electrons are described by the wave function (the surface is to the right),

$$\Psi^{\mathrm{inc}}(\boldsymbol{r}) = \exp(\mathrm{i}\boldsymbol{K}^{+}\cdot\boldsymbol{r}), \tag{2.1}$$

where

$$\boldsymbol{K}^{+} = (\boldsymbol{k}_{\parallel}, k_z^{+}), \qquad k_z^{+} = +\sqrt{2E - |\boldsymbol{k}_{\parallel}|^2}. \tag{2.2}$$

$\boldsymbol{k}_{\parallel}$ is the component of the wave vector parallel to the surface, a good quantum number to within surface reciprocal lattice vectors $\boldsymbol{G}$, and E is the electron energy. The electrons are multiply scattered by the surface and substrate crystal through the surface reciprocal lattice vectors, resulting in the reflected waves,

$$\Psi^{\mathrm{ref}}(\boldsymbol{r}) = \sum_{\boldsymbol{G}} A_{\boldsymbol{G}} \exp(\mathrm{i}\boldsymbol{K}_{\boldsymbol{G}}^{-}\cdot\boldsymbol{r}), \tag{2.3}$$

with

$$\boldsymbol{K}_{\boldsymbol{G}}^{-} = (\boldsymbol{k}_{\parallel} + \boldsymbol{G}, k_z^{-}), \qquad k_z^{-} = -\sqrt{2E - |\boldsymbol{k}_{\parallel} + \boldsymbol{G}|^2}. \tag{2.4}$$

Downloaded from rsta.royalsocietypublishing.org

It is the $|A_{\boldsymbol{G}}|^2$ that are measured in LEED experiments, and it is the task of LEED theory to calculate these diffraction spot intensities.

LEED calculations are carried out within a single-particle framework, in which the elastically scattered electron feels a complex self-energy due to the electron–electron interaction, as well as the Hartree potential due to the smeared-out charge density of the other electrons, and the nuclear potential (Van Hove *et al*. 1986). The real part of the self-energy results in shifts of the single-particle energy levels, and the imaginary part gives rise to lifetime broadening. Outside the solid an electron feels an effective potential that has the asymptotic image form (Lang & Kohn 1970):

$$V^{\mathrm{eff}}(\boldsymbol{r}) \sim -\frac{1}{4|z-z_0|}. \tag{2.5}$$

Here z_0 is the image plane from which the image potential is measured. The way in which V^{eff} approaches the asymptotic form, and the actual value of z_0, depend on the energy of the electron (Echenique & Pendry 1975). This is because the image potential results from the dynamic response of the electrons, which of course depends on the velocity of the external electron. Very recently, there have been *ab initio* calculations of V^{eff} both for jellium (Eguiluz *et al*. 1992) and for Al (White *et al*. 1998), for electrons with an energy close to the vacuum zero. In fact, in most LEED calculations it is assumed that the electron feels a constant potential outside the crystal (Van Hove *et al*. 1986), with a step at the surface (though some resonance structure does involve the image potential (Jennings & Jones 1986)). Inside the solid the self-energy is usually taken in LEED work to be a constant added on to the potential from density-functional theory, and is found by fitting to the experimental spectra.

To calculate the reflection coefficients $A_{\boldsymbol{G}}$ in (2.3) we solve the Schrödinger equation for electrons in the crystal potential, matching the solution inside the solid onto the incident and scattered waves. This procedure is most conveniently carried out within the framework of layer scattering, in which the solid is divided up into layers of atoms and then the scattering properties of each layer are found by two-dimensional, multiple-scattering theory (Pendry 1994). In between the layers, the potential is taken to be a constant $V_{0\mathrm{r}}$ (the real part of the inner potential) (Saldin & Spence 1994), so that the LEED wave function in this region propagates as a sum of the plane waves with energy $E - V_{0\mathrm{r}}$ and reduced two-dimensional wave vector $\boldsymbol{k}_{\|}$ (the reduced wave vector means the wave vector brought inside the surface-parallel Brillouin zone by adding on a surface reciprocal lattice vector). Specifically, in the region between the nth and $(n+1)$th atomic layers we have (Pendry 1994)

$$\Psi(\boldsymbol{r}) = \sum_{\boldsymbol{G}} \{a^{+}_{n,\boldsymbol{G}} \exp[\mathrm{i}\hat{\boldsymbol{K}}^{+}_{\boldsymbol{G}} \cdot (\boldsymbol{r} - n\boldsymbol{c})] + a^{-}_{n,\boldsymbol{G}} \exp[\mathrm{i}\hat{\boldsymbol{K}}^{-}_{\boldsymbol{G}} \cdot (\boldsymbol{r} - n\boldsymbol{c})]\}, \tag{2.6}$$

where the wave vectors are given by

$$\hat{\boldsymbol{K}}^{\pm}_{\boldsymbol{G}} = (\boldsymbol{k}_{\|} + \boldsymbol{G}, \hat{k}^{\pm}_{z}), \qquad \hat{k}^{\pm}_{z} = \pm\sqrt{2(E - V_{0\mathrm{r}}) - |\boldsymbol{k}_{\|} + \boldsymbol{G}|^2}. \tag{2.7}$$

Here $\boldsymbol{c}$ is the stacking vector that takes us from one layer to the next. $\hat{k}^{\pm}_{z}$ can be imaginary, so that (2.6) includes exponentially increasing and decreasing waves as well as propagating waves. The coefficients $a^{\pm}_{n,\boldsymbol{G}}$ are related to $a^{\pm}_{n+1,\boldsymbol{G}}$ and $a^{\pm}_{n-1,\boldsymbol{G}}$ on either side by the reflection and transmission properties of the nth layer, and by adding successive layers the reflection coefficients of the whole stack of layers making

Downloaded from rsta.royalsocietypublishing.org

up the semi-infinite solid can be calculated. This procedure converges rapidly due to the damping introduced by the imaginary part of the inner potential.

Numerous structures of ordered surfaces have been determined by fitting experimental LEED spectra with calculations along the lines we have just indicated (Rous 1995*b*). However, many adsorbate systems are disordered (Van Hove & Somorjai 1994), and the methodology of diffuse LEED has been set up to determine the geometry of adsorbates without two-dimensional periodicity (Pendry & Saldin 1984; Heinz *et al.* 1985; Saldin *et al.* 1985). Let us consider the scattering by a single adsorbate molecule on top of an otherwise perfect semi-infinite crystal. If t is the T-matrix for scattering from the adsorbate by itself, and T for scattering from the clean surface, the T-matrix for the combined system is given by

$$T_{\mathrm{comb}} = t + T + tG_0T + TG_0t + \cdots, \tag{2.8}$$

where G_0 is the free-electron Green function. Note that the definition of the T-matrix restricts the series, so that adjacent ts or Ts cannot appear. This can be rewritten as

$$T_{\mathrm{comb}} = T + (1 + TG_0)\tau(1 + G_0T), \tag{2.9}$$

where τ, the adsorbate scattering path operator (Gonis 1992), describes all scatterings that start and finish on the adsorbate, including scattering paths through the substrate:

$$\tau = t + tG_0TG_0t + \cdots. \tag{2.10}$$

The transition amplitude for scattering from an incident plane wave $\exp(\mathrm{i}\boldsymbol{k}\cdot\boldsymbol{r})$ to $\exp(\mathrm{i}\boldsymbol{k}'\cdot\boldsymbol{r})$ is then given by

$$\langle\boldsymbol{k}'|T_{\mathrm{comb}}|\boldsymbol{k}\rangle = \langle\boldsymbol{k}'|T|\boldsymbol{k}\rangle + \langle\boldsymbol{k}'(1 + TG_0)|\tau|(1 + G_0T)\boldsymbol{k}\rangle. \tag{2.11}$$

The first term describes scattering from the clean surface, and is zero except when the surface-parallel components of $\boldsymbol{k}$ and $\boldsymbol{k}'$ differ by a surface reciprocal lattice vector. The second term gives rise to the diffuse scattering in all directions, and we can consider it as the transition amplitude between

$$|\psi^+_{\boldsymbol{k}}\rangle = (1 + G_0T)|\boldsymbol{k}\rangle \quad \text{and} \quad |\psi^-_{\boldsymbol{k}'}\rangle = (1 + G_0^\dagger T^\dagger)|\boldsymbol{k}'\rangle.$$

$|\psi^+_{\boldsymbol{k}}\rangle$ is the LEED wave function arising from scattering $\exp(\mathrm{i}\boldsymbol{k}\cdot\boldsymbol{r})$ off the clean surface, and $|\psi^-_{\boldsymbol{k}'}\rangle$ is the time-reversed LEED wave function corresponding to $\exp(\mathrm{i}\boldsymbol{k}'\cdot\boldsymbol{r})$; we let $\exp(-\mathrm{i}\boldsymbol{k}'\cdot\boldsymbol{r})$ scatter off the surface and then take the complex conjugate. The transition between these LEED states is caused by τ.

This result for the diffuse scattering from an adsorbate is straightforward to evaluate (Pendry & Saldin 1984); we have seen at the beginning of this section how the LEED initial and final states in (2.11) can be constructed. The scattering path operator τ can be found from a multiple scattering calculation for the cluster consisting of the adsorbate plus the adjacent substrate. The short mean free path restricts the amount of substrate that needs to be included. The potential is generally assumed to have muffin-tin form, i.e. spherically symmetric within a muffin-tin sphere around each atom with a constant potential in between. With this simple form of potential, τ can then be found very efficiently.

In ordered LEED the intensities of the discrete diffracted beams (the I/V spectra) are studied as a function of electron energy; in diffuse LEED the entire diffuse scattering pattern is measured at fixed electron energy and compared with calculation

Downloaded from rsta.royalsocietypublishing.org

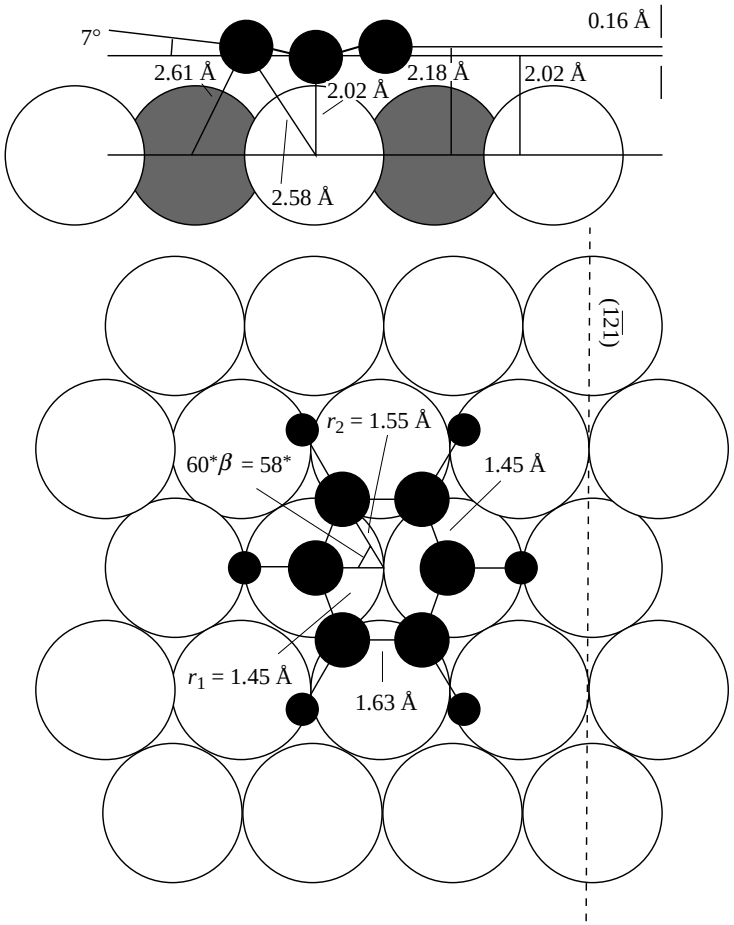

Figure 1. Disordered benzene on Pt(111), showing distortions from the gas-phase benzene geometry (Wander *et al*. 1991).

(Heinz *et al*. 1985). Quasi-elastic diffuse scattering can also result from phonons at the surface, and to remove this the diffuse LEED pattern of the clean substrate is subtracted from that of the adsorbate system (Wander *et al*. 1991). Complicated adsorbates can now be studied (Van Hove & Somorjai 1994), for example, disordered benzene on the Pt(111) surface (Wander *et al*. 1991); a systematic study of hydrocarbon adsorbates is fundamental for understanding petrochemical catalysis. By systematically comparing the measured and calculated diffuse LEED patterns (a somewhat different method of calculating the scattering from the τ-method described above was actually used for the analysis), it has been found that the benzene chemisorbs in two-fold bridge sites with a buckling distortion of the benzene ring (figure 1) (Wander *et al*. 1991).

3. Theory of high-resolution electron energy loss spectroscopy

Inelastic losses of low-energy electrons scattering from surfaces can be used to probe vibrational modes and electronic excitations in adsorbates (Palmer & Rous 1992).

Downloaded from rsta.royalsocietypublishing.org

In this section, we shall mainly concentrate on adsorbate vibrations where the excitations have an energy of typically 100 meV, though much of the formalism we shall outline can be extended to study the other surface excitations. Using high-resolution electron energy loss spectroscopy (HREELS), the vibrational losses can be studied with an energy resolution of *ca.* 10 meV.

There are two ways in which the scattering electron can interact with the vibrating atoms (Palmer & Rous 1992; Aers *et al.* 1981; Aers & Pendry 1982): first, long-range dipole scattering in which the electron is scattered by the dipole field produced by the dynamic effective charges on the displaced atoms; and, second, impact scattering in which the electron interacts at close range with the core potential of the displaced atoms. Dipole scattering gives an intense lobe in the specular direction, whereas impact scattering is more isotropic, and this enables the two to be distinguished (Bare *et al.* 1983). Resonance scattering is well known in electron scattering from molecules in the gas phase, and it is also observed in inelastic scattering from adsorbed molecules (Palmer & Rous 1992; Jones *et al.* 1989; Jensen *et al.* 1990); an electron scattering at the resonance energy becomes trapped for a time in an excited state, and the change in the interatomic potential in the negative molecular ion results in enhancement of vibrational losses. This is really a special case of impact scattering, but is particularly interesting because the angular distribution of the scattered electrons reflects the geometry of the resonance orbital (Palmer & Rous 1992).

The transition amplitude for inelastic scattering of electrons by surface adsorbates has a similar structure to (2.11), involving the LEED initial state and the time-reversed LEED final state (Aers *et al.* 1981; Aers & Pendry 1982). An important difference is that we are usually interested in a single inelastic scattering event, so τ is replaced by the first term in the series (2.10). The amplitude for scattering electrons inelastically from plane wave $\exp(\mathrm{i}\boldsymbol{k}\cdot\boldsymbol{r})$ to $\exp(\mathrm{i}\boldsymbol{k}'\cdot\boldsymbol{r})$, due to a transition from state ν to ν' in the adsorbate, is then given by

$$f(\boldsymbol{k}',\nu'\leftarrow\boldsymbol{k},\nu)\propto\langle\psi^-_{\boldsymbol{k}'}|t^{\nu'\nu}|\psi^+_{\boldsymbol{k}}\rangle. \tag{3.1}$$

$t^{\nu'\nu}$ is the inelastic T-matrix for scattering from the adsorbate, producing a transition between the LEED states $|\psi^+_{\boldsymbol{k}}\rangle$ and $|\psi^-_{\boldsymbol{k}'}\rangle$. The LEED states describe elastic scattering from the whole system, including the adsorbates themselves. The inelastic scattering breaks the coherence, so it adds incoherently from the separate adsorbates.

An early application of this LEED approach to inelastic scattering was to the angular distribution of the inelastically scattered electrons from vibrational modes of H adsorbed on W(001) (Bare *et al.* 1983). Three normal vibrational modes of the H atoms are measured in HREELS experiments: the symmetric stretching of the H against the surface produces a dynamic dipole and dominates the specular scattering, whereas the wagging and asymmetric stretch modes are excited by impact scattering. To calculate the impact scattering, the inelastic T-matrix was found by displacing the H muffin-tin potential (the heavy W atoms hardly move), and the initial and final LEED states were also evaluated with muffin-tin potentials. Excellent agreement was obtained for the angular variation of inelastic scattering.

To describe resonance scattering from an adsorbed molecule, it is often convenient to use an angular momentum representation of the initial and final states about the molecule:

$$f(\boldsymbol{k}',\nu'\leftarrow\boldsymbol{k},\nu)\propto\sum_{lm,l'm'}\langle\psi^-_{\boldsymbol{k}'}|l'm'\rangle\langle l'm'|t^{\nu'\nu}|lm\rangle\langle lm|\psi^+_{\boldsymbol{k}}\rangle. \tag{3.2}$$

Downloaded from rsta.royalsocietypublishing.org

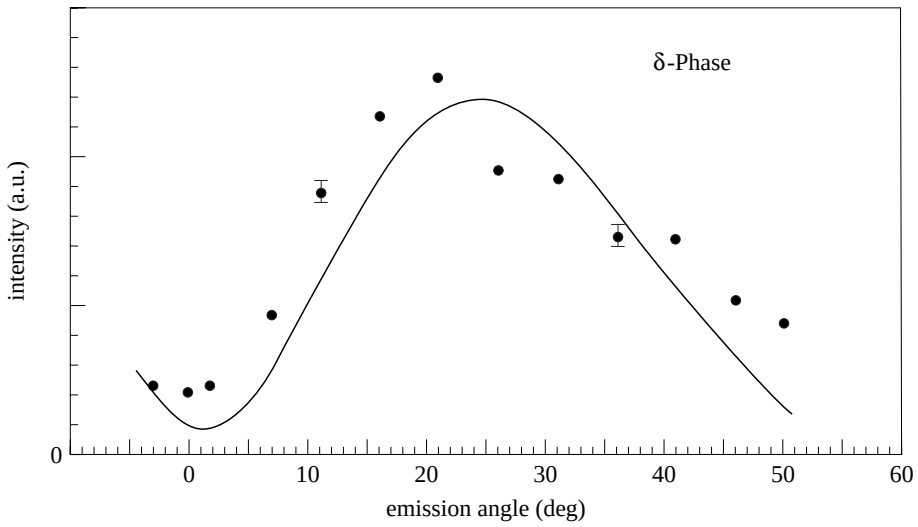

Figure 2. Angular distribution (dots) of electrons scattered by O_2 physisorbed on graphite, resonance scattering after exciting the $\nu = 0 \rightarrow 1$ vibrational transition in O_2. Electron energy is 8.5 eV, at an angle of incidence of 60°; angles are measured from the surface normal. Solid line shows calculated angular distribution, with a molecular tilt of 15° from the surface (Jensen *et al*. 1990).

A single partial wave often dominates in the capture and emission of the electron from the resonance (Rous *et al*. 1989; Davenport *et al*. 1978), and the inelastic T-matrix in (3.2) simplifies to

$$\langle l'm'|t^{\nu'\nu}|lm\rangle \approx \langle l'm'|t^{\nu'\nu}|lm\rangle\delta_{lm,l'm'}. \tag{3.3}$$

The scattering process picks out this partial wave in both the initial and final states:

$$f(\boldsymbol{k}', \nu' \leftarrow \boldsymbol{k}, \nu) \propto \langle\psi^-_{\boldsymbol{k}'}|lm\rangle\langle lm|t^{\nu'\nu}|lm\rangle\langle lm|\psi^+_{\boldsymbol{k}}\rangle. \tag{3.4}$$

In the $^4\Sigma_u$ resonance in O_2, at 9.5 eV in the free molecule, the dominant component in the wave function of the scattering electron has pσ symmetry (Palmer & Rous 1992). The transition amplitude for inelastic scattering via this resonance then has the following angular variation in the case of the free molecule,

$$f(\boldsymbol{k}', \nu' \leftarrow \boldsymbol{k}, \nu) \propto \cos\theta_i \cos\theta_f, \tag{3.5}$$

where the angle of incidence θ_i and the angle of scattering θ_f are measured from the molecular axis. When O_2 is physisorbed on graphite, the same resonance is seen in HREELS from the O_2 vibrational modes at an electron energy of 8.5 eV (Jensen *et al*. 1990). The variation in transition amplitude with incidence and scattering angles can then be found by calculating the LEED states corresponding to these angles and then picking out the $(l = 1, m = 0)$ partial wave in the expansion about the molecule. By comparing theory with experiment, the angle of tilt of the O_2 molecules from the surface has been found (figure 2) (Jensen *et al*. 1990).

The resonance energy of the scattering electron is lowered when the molecule is physisorbed, compared with resonance in the free molecule, due to the interaction with the image potential (Palmer & Rous 1992). The resonance is also broadened

Downloaded from rsta.royalsocietypublishing.org

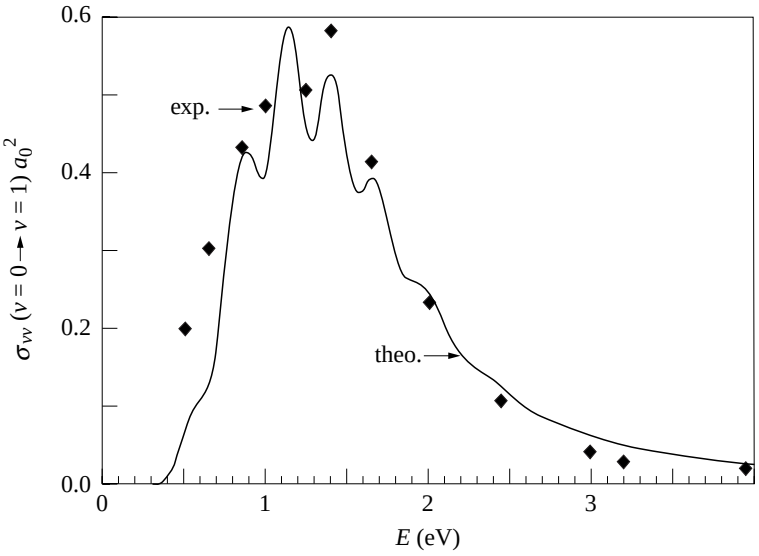

Figure 3. Cross-section for electrons scattered by N_2 physisorbed on Ag(111), after exciting the $\nu = 0 \rightarrow 1$ vibrational transition in N_2, as a function of incident electron energy. Solid line shows calculated intensity, and diamonds experiment (Demuth *et al.* 1981).

by physisorption, due to the surface reducing the symmetry and opening up new decay channels. Multiple scattering can be used to study the resonance energy and lifetime (Gerber & Herzenberg 1985); the expression for the adsorbate scattering path operator (2.10) can be rewritten as

$$\tau = t(1 - G_0 T G_0 t)^{-1}, \tag{3.6}$$

where all the surface information is in T and the molecule is described by t. The condition for a resonance is a root at complex energy E of

$$\det(1 - G_0 T G_0 t) = 0. \tag{3.7}$$

The real part of E is the resonance energy, and the imaginary part is the width (i.e. the inverse lifetime). Using this approach the energy and lifetime of the $^4\Sigma_u$ resonance of O_2 adsorbed on Ag(110) have been studied for different adsorption sites and as a function of the height of the molecule above the surface (Rous 1995*a*). The LKKR method was used to find T, with a muffin-tin potential describing the atoms and a parametrized surface barrier potential. The muffin-tin form of potential was also used to find t. It was found that as well as the general effects of the surface on the resonance described above, the surface electronic structure has an important effect in reducing the lifetime.

A completely different approach to inelastic electron scattering is the coupled angular modes (CAM) method, in which a spherical harmonic expansion is used to describe the electron wave function (Gauyacq *et al.* 1997). The system is divided into two regions: an internal region defined by a sphere of radius r_c and an external region that comprises all space outside this sphere. The electron–molecule scattering in the external region is described by a superposition of polarization and centrifugal potentials denoted by V_{lm}^{ext} and a shifted image potential V_S which represents the electron–surface interaction. In the internal region, the electron–molecule potential

Downloaded from rsta.royalsocietypublishing.org

is not calculated explicitly but is represented by specifying the logarithmic derivative of the incident electron wave function at $r = r_c$. This logarithmic derivative, which acts as boundary condition for the external region solution, can either be extracted from *ab initio* calculations or adjusted to reproduce experimental results. The wave function for the system is expanded in the form (Djamo *et al.* 1995),

$$\Psi(\boldsymbol{r}, R) = \sum_{\nu} \sum_{lm} \frac{1}{r} F^{\nu}_{lm}(r) Y_{lm}(\Omega) \chi_{\nu}(R), \tag{3.8}$$

where (r, Ω) are the electron coordinates and $\chi_\nu(R)$ is the νth vibrational wave function of the molecule. Then in the external region the electron wave function satisfies

$$-\frac{1}{2}\frac{\mathrm{d}^2 F^{\nu}_{lm}}{\mathrm{d}r^2} + V^{\mathrm{ext}}_{lm}(r) F^{\nu}_{lm}(r) + \sum_{l'} \langle lm | V_{\mathrm{S}} | l'm' \rangle F^{\nu}_{l'm'}(r) = E F^{\nu}_{lm}. \tag{3.9}$$

The solution of these coupled equations together with the boundary conditions yields the scattering matrix for the problem. The method is slowly convergent and, rather than calculating the differential cross-section, partial cross-sections are calculated by integrating over either the vacuum or substrate half-space. Results obtained with the CAM method for the cross-section for resonant excitation of vibrational excitations in N_2 physisorbed on Ag are shown in figure 3 (Djamo *et al.* 1995).

The excitation proceeds via the $^2\Sigma_g$ shape resonance involving the dπ partial wave $(l = 2, m = 1)$. The oscillations are the remnants of the 'boomerang' oscillations that are an interference effect occurring when the lifetime of the resonance is comparable with the period of oscillation. At the surface the resonance lifetime is reduced, and this smears out the oscillations. Agreement with experiment is rather good (Demuth *et al.* 1981).

4. R-matrix formalism

We now consider the developments currently underway to describe electron scattering by physisorbed diatomic molecules within the R-matrix formulation, which removes some of the approximations made in the CAM method discussed above. We approximate a jellium metal surface by a shifted image potential of the form,

$$\left.\begin{aligned} V_{\mathrm{S}}(z) &= \frac{-c}{Z_0 - z + d}, & z > d, \\ V_{\mathrm{S}}(z) &= \frac{-c}{Z_0}, & z < d, \end{aligned}\right\} \tag{4.1}$$

where c and Z_0 are constants related to the work potential of the surface and d is the distance from the surface of the centre of gravity of the molecule. Structureless jellium is a widely used model for representing surface adsorption, especially on s–p bonded metals (Trioni *et al.* 1996). The image potential is expressed as an infinite sum over Legendre polynomials about the normal to the surface z (see figure 4) such that

$$V_{\mathrm{S}}(z) = \sum_{\lambda=0}^{\infty} V_\lambda(r) P_\lambda(\cos\theta), \tag{4.2}$$

Downloaded from rsta.royalsocietypublishing.org

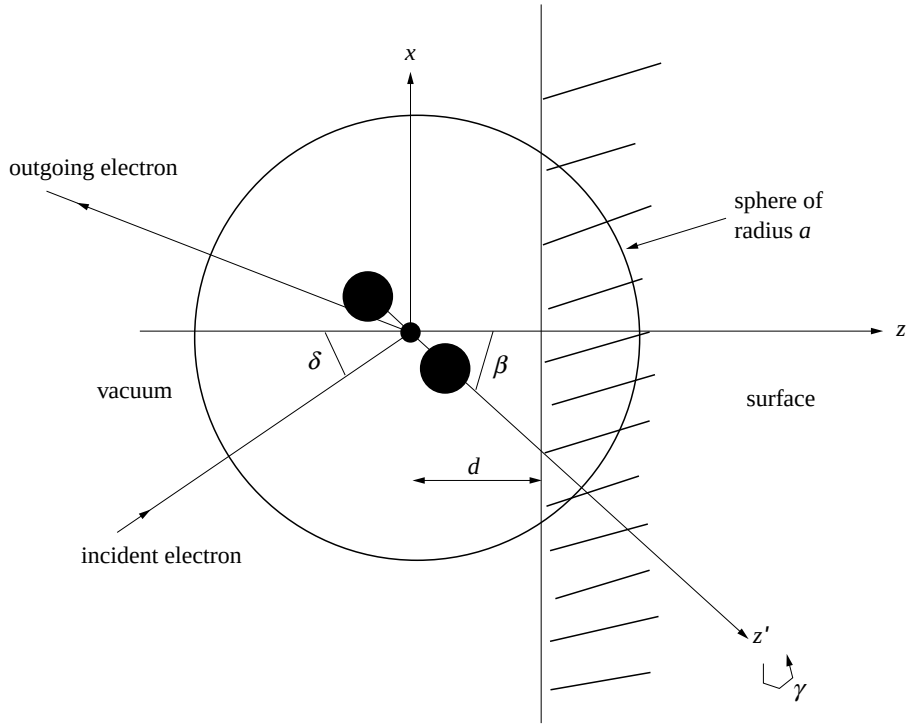

Figure 4. Electron-adsorbed molecule system.

where the expansion coefficients V_λ depend only on the radial distance r from the molecular centre of gravity.

The internuclear axis z' of the molecule is usually chosen as the quantization axis for the sake of computational convenience. The surface potential about this axis is given by

$$V_{\mathrm{S}}(z) = \sum_{\lambda=0}^{\infty} V_\lambda(r)\left(\frac{4\pi}{2\lambda+1}\right)^{1/2} \sum_{m=-\lambda}^{\lambda} \mathcal{D}_{m0}(\alpha,\beta,\gamma) Y_{\lambda m}(\theta',\phi'), \tag{4.3}$$

where (θ',ϕ') refer to the molecular frame. $\mathcal{D}_{m0}(\alpha,\beta,\gamma)$ denotes the rotation D-matrix where the angles α,β and γ are the Euler rotations required to bring the laboratory axes onto the molecular axes.

We proceed in the usual way by dividing configuration space into two regions: an internal region defined by $r_i \leqslant a$, for all i, where r_i is the distance of the ith electron to the centre of gravity of the molecule; and an external region where the radial coordinate, r_{N+1}, of the scattered electron is greater than a. The value a is chosen so that all the target states of interest are encompassed entirely within the internal region. Here the scattered electron lies within the charge cloud of the target, requiring the inclusion of electron exchange and short-range correlation effects in the total wave function. In the external region, these effects are negligible and may be omitted from the wave function description without compromising the accuracy of the overall result.

Downloaded from rsta.royalsocietypublishing.org

(*a*) *Internal region*

The internal region wave function is expanded in terms of members, ψ_k, of a complete basis. Initially, we assume that the ψ_k depend parametrically on the internuclear separation, which is assumed to be constant throughout the calculation. The ψ_k are defined as

$$\psi_k(\boldsymbol{x}_1,\ldots,\boldsymbol{x}_{N+1}) = \sum_i \sum_j \mathcal{A}\overline{\Phi}_i(\boldsymbol{x}_1,\ldots,\boldsymbol{x}_N,\sigma_{N+1})\eta_j(\boldsymbol{r}_{N+1})c_{ijk} + \sum_i \chi_i(\boldsymbol{x}_1,\ldots,\boldsymbol{x}_{N+1})b_{ik}, \quad (4.4)$$

where $\boldsymbol{x}_i = (\boldsymbol{r}_i, \sigma_i)$ is the space-spin coordinate of the ith electron and $\mathcal{A}$ is the usual antisymmetrization operator that antisymmetrizes the $(N+1)$th electron coordinate with the coordinates of all the other electrons.

The $\overline{\Phi}_i$ in the first expansion of (4.4) are formed by coupling the electronic wave function Φ_i for the target with the spin function of the scattered electron to form eigenfunctions of S^2 and S_z, where S and S_z are, respectively, the total spin angular momentum operator and its projection onto the quantization axis, z'.

The target wave functions Φ_i are represented as a sum of N electron configurations ϕ_j such that

$$\Phi_i(\boldsymbol{x}_1,\ldots,\boldsymbol{x}_N) = \sum_j \phi_j(\boldsymbol{x}_1,\ldots,\boldsymbol{x}_N)d_{ij}. \quad (4.5)$$

The configurations ϕ_j are themselves formed from bound molecular orbitals that are vanishingly small by the boundary of the inner region. The coefficients d_{ij} in equation (4.5) are obtained by diagonalizing the operator

$$\left(H_N + \sum_{i=1}^{N} V_{\mathrm{S}}(z_i)\right)$$

such that

$$\left\langle \Phi_i \middle| H_N + \sum_{i=1}^{N} V_{\mathrm{S}}(z_i) \middle| \Phi_j \right\rangle = E_i^N \delta_{ij}, \quad (4.6)$$

where H_N is Born–Oppenheimer Hamiltonian for the N-electron system and $V_{\mathrm{S}}(z_i)$ denotes the surface potential operator given by equation (4.3) acting on the ith electron. E_i^N is the energy of the Φ_i target state.

The $\eta_j(\boldsymbol{r}_{N+1})$ in equation (4.4) are continuum orbitals describing the motion of the scattered electron inside the inner region, where the values of these functions are non-zero at the boundary $r = a$. They are constructed such that they are orthogonal to the bound orbitals and have exactly the same form as used in electron scattering by gas-phase molecules (Burke *et al.* 1977).

Turning our attention to the second summation in the expansion of the ψ_k given by equation (4.4), the $\chi_i(\boldsymbol{x}_1,\ldots,\boldsymbol{x}_{N+1})$ are $(N+1)$-electron configurations constructed entirely from bound molecular orbitals. They serve a dual purpose: firstly, they take account of that part of configuration space which has been omitted owing to the imposed orthogonality between the bound and continuum orbitals; secondly, they help to describe short-range correlation effects including virtual excitations to

Downloaded from rsta.royalsocietypublishing.org

electronic states not included in the first summation of the equation. Finally, the coefficients b_{ik} and c_{ijk} are uniquely determined by requiring that

$$\left\langle \psi_k \middle| H_{N+1} + \sum_{i=1}^{N+1} V_{\mathrm{S}}(z_i) \middle| \psi_{k'} \right\rangle = E_k \delta_{kk'}, \tag{4.7}$$

where H_{N+1} is the Born–Oppenheimer Hamiltonian for the $(N+1)$-electron system and $V_{\mathrm{S}}(z_i)$ is the surface potential. The eigenvalues E_k and eigenvectors given by equation (4.7) are then used to construct the R-matrix at the boundary of the internal region. This R-matrix is then rotated from the molecular frame back into the laboratory frame. The final R-matrix, which we denote $\boldsymbol{R}^{\boldsymbol{u}}(a)$, defines the logarithmic derivative of the total wave function at the edge of the internal region and acts as the boundary condition for the solution in the external region.

(*b*) *External region*

In the external region, we express the total wave function $\Psi^{\mathrm{tot}}(\boldsymbol{r})$ as

$$\Psi^{\mathrm{tot}}(\boldsymbol{r}) = \Psi^{\mathrm{inc}}(\boldsymbol{r}) + \Psi^{\mathrm{scatt}}(\boldsymbol{r}), \qquad r > a, \tag{4.8}$$

where $\boldsymbol{r}$ is the coordinate of the scattered electron. $\Psi^{\mathrm{inc}}(\boldsymbol{r})$ denotes that part of the wave function corresponding to the probe electron incident upon the surface in the absence of the molecule. For an electron incident with momentum $\boldsymbol{k}$, at any arbitrary angle δ relative to the surface, $\Psi^{\mathrm{inc}}(\boldsymbol{r})$ satisfies the Schrödinger equation,

$$(\nabla^2_{\boldsymbol{r}} - 2V_{\mathrm{S}}(z) + k^2)\Psi^{\mathrm{inc}}(\boldsymbol{r}) = 0, \tag{4.9}$$

which can be solved trivially numerically to obtain $\Psi^{\mathrm{inc}}(\boldsymbol{r})$ over all space. Ψ^{scatt} is that part of the total wave function specifically due to scattering by the adsorbed molecule. The asymptotic form of Ψ^{scatt} yields the scattering amplitude from which all the scattering information may be derived. Making a partial wave expansion of Ψ^{tot}, Ψ^{inc} and Ψ^{scatt} we have

$$\left.\begin{aligned} \Psi^{\mathrm{tot}}(\boldsymbol{r}) &= \sum_{lm}^{\infty} r^{-1} u_{lm}(r) Y_{lm}(\hat{\boldsymbol{r}}), \\ \Psi^{\mathrm{inc}}(\boldsymbol{r}) &= \sum_{lm}^{\infty} r^{-1} v_{lm}(r) Y_{lm}(\hat{\boldsymbol{r}}), \\ \Psi^{\mathrm{scatt}}(\boldsymbol{r}) &= \sum_{lm}^{\infty} r^{-1} x_{lm}(r) Y_{lm}(\hat{\boldsymbol{r}}). \end{aligned}\right\} \tag{4.10}$$

The $Y_{lm}(\hat{\boldsymbol{r}})$ are the usual spherical harmonics referred to the laboratory axes. Substituting equation (4.10) into equation (4.8) and projecting onto the spherical harmonics, we obtain

$$x_{lm}(r) = u_{lm}(r) - v_{lm}(r). \tag{4.11}$$

If we consider the electron–molecule interaction, it becomes clear that as the value of l increases the centrifugal barrier becomes sufficiently large to ensure that the probe electron is 'pushed' outside the molecular charge cloud and is scattered by

Downloaded from rsta.royalsocietypublishing.org

the surface potential alone. Consequently, above a certain value of l, which we shall denote as l_0, Ψ^{scatt} is zero, and hence

$$u_{lm}(r) = v_{lm}(r), \qquad x_{lm}(r) = 0, \qquad l > l_0. \tag{4.12}$$

In the external region, $\Psi^{\mathrm{scatt}}(\boldsymbol{r})$ satisfies exactly the same equation as $\Psi^{\mathrm{inc}}(\boldsymbol{r})$ if we neglect the long-range polarization potential of the molecule. That is,

$$(\nabla^2 - 2V_{\mathrm{S}}(z) + k^2)\Psi^{\mathrm{scatt}} = 0, \qquad r \geqslant a. \tag{4.13}$$

Using equations (4.2) and (4.10) and projecting equation (4.13) onto the spherical harmonics $Y_{lm}(\hat{\boldsymbol{r}})$, we obtain a set of $(l_0 + 1 - m)$ coupled differential equations for the $x_{lm}(r)$ given by

$$\left(\frac{\mathrm{d}^2}{\mathrm{d}r^2} - \frac{l(l+1)}{r^2} + k^2\right)x_{lm}(r) = 2\sum_{l'=m}^{l_0} V^s_{lml'm}(r)x_{l'm}(r), \qquad r \geqslant a, \tag{4.14}$$

where the coupling potential matrix $V^s_{lml'm}(r)$ is defined as

$$V^s_{lml'm}(r) = \sum_{\lambda} V_\lambda(r) \int Y^*_{lm}(\hat{\boldsymbol{r}})P_\lambda(\cos\theta)Y_{l'm}(\hat{\boldsymbol{r}})\,\mathrm{d}\hat{\boldsymbol{r}}. \tag{4.15}$$

We solve these equations subject to the outgoing wave boundary condition given by

$$\Psi^{\mathrm{scatt}}(\boldsymbol{r}) \underset{r\to\infty}{\sim} \sum_{lm} f_{lm}(\theta,\phi)\frac{\exp(\mathrm{i}K_{lm}(r))}{r}, \tag{4.16}$$

where the quantity $f_{lm}(\theta,\phi)$ is the scattering amplitude, which depends implicitly through matching conditions on the angle δ of the incident electron. Writing (4.14) in matrix form, we obtain

$$\left(\frac{\mathrm{d}^2}{\mathrm{d}r^2} + \boldsymbol{V}^{\mathrm{tot}}_m(r) + \boldsymbol{k}^2\right)\boldsymbol{x}_m(r) = 0, \qquad r \geqslant a, \tag{4.17}$$

where

$$\boldsymbol{V}^{\mathrm{tot}}_m(r) = \frac{-l(l+1)}{r^2}\delta_{ll'} - 2V^s_{lml'm}(r), \qquad r \geqslant a. \tag{4.18}$$

Diagonalizing this potential matrix by an orthogonal transformation as follows,

$$\boldsymbol{A}^{\mathrm{T}}_m(r)\boldsymbol{V}^{\mathrm{tot}}_m(r)\boldsymbol{A}_m(r) = \boldsymbol{D}_m(r), \tag{4.19}$$

and writing

$$\boldsymbol{g}_m(r) = \boldsymbol{A}^{\mathrm{T}}_m(r)\boldsymbol{x}_m(r), \tag{4.20}$$

we may express equation (4.17) as

$$\left(\boldsymbol{A}^{\mathrm{T}}_m(r)\frac{\mathrm{d}^2}{\mathrm{d}r^2}\boldsymbol{A}_m(r) + \boldsymbol{D}_m(r) + \boldsymbol{k}^2\right)\boldsymbol{g}_m(r) = 0, \qquad r \geqslant a. \tag{4.21}$$

By fitting both the diagonal matrix $\boldsymbol{D}_m(r)$ and the transformation matrix $\boldsymbol{A}_m(r)$ to an inverse multipole expansion in r, it can be shown that equation (4.21) has the asymptotic form,

$$\left(\frac{\mathrm{d}^2}{\mathrm{d}r^2} + \frac{\boldsymbol{q}_m}{r} + \boldsymbol{P}^2_m + O(r^{-2})\right)\boldsymbol{g}_m(r) = 0, \qquad r \geqslant b \gg a. \tag{4.22}$$

Downloaded from rsta.royalsocietypublishing.org

The $\boldsymbol{q}_m$ and $\boldsymbol{P}_m^2$ are diagonal matrices that depend on m, and b is the radius at which the external region equations reach their asymptotic form. We look for outgoing wave solutions of the form,

$$\boldsymbol{g}_m(r) = \exp(\mathrm{i}\boldsymbol{K}_m(r))\boldsymbol{N}_m, \qquad r \geqslant b, \tag{4.23}$$

where $\boldsymbol{N}_m$ is an undetermined normalization vector and $\boldsymbol{K}_m(r)$ is a diagonal matrix defined by

$$\boldsymbol{K}_m(r) = \boldsymbol{P}_m r + \frac{\boldsymbol{q}_m}{2\boldsymbol{P}_m}\ln(2\boldsymbol{P}_m r). \tag{4.24}$$

Using expression (4.20), we obtain a matrix of solutions $\boldsymbol{X}_m(r)$ of equation (4.17) where

$$\boldsymbol{X}_m(r) = \boldsymbol{A}_m(r)\exp(\mathrm{i}\boldsymbol{K}_m(r))\boldsymbol{N}_m = \boldsymbol{x}_m(r)\boldsymbol{N}_m. \tag{4.25}$$

The corresponding R-matrix, which defines the logarithmic derivative of $\boldsymbol{x}_m$, is given by

$$\begin{aligned}\boldsymbol{R}_m^{\boldsymbol{x}}(b) &= \boldsymbol{X}_m(b)\left[b\frac{\mathrm{d}}{\mathrm{d}r}\boldsymbol{X}_m(b)\right]^{-1}_{r=b}\\ &= \boldsymbol{x}_m(b)\left[b\frac{\mathrm{d}}{\mathrm{d}r}\boldsymbol{x}_m(b)\right]^{-1}_{r=b}.\end{aligned} \tag{4.26}$$

Clearly, the R-matrix defined by (4.26) has been derived for fixed m. However, in the general case where the molecule is orientated at an arbitrary angle relative to the surface, m is not conserved. In order that this property is included in the external region equations, we obtain the R-matrices $\boldsymbol{R}_m^{\boldsymbol{x}}(b)$ for $(-l_0 \leqslant m \leqslant l_0)$. These are then used to construct the 'super' R-matrix $\boldsymbol{R}^{\boldsymbol{x}}(b)$, which is block diagonal with the matrices $\boldsymbol{R}_m^{\boldsymbol{x}}(b)$ forming the diagonal blocks.

The super R-matrix is then propagated backwards using the procedure of Baluja *et al.* (1982) to obtain the corresponding R-matrix $\boldsymbol{R}^{\boldsymbol{x}}(a)$ on the boundary of the internal region. We have

$$\begin{aligned}\boldsymbol{R}^{\boldsymbol{x}}(a) &= \boldsymbol{x}(a)\left[a\frac{\mathrm{d}}{\mathrm{d}r}\boldsymbol{x}(a)\right]^{-1}_{r=a}\\ &= (\boldsymbol{u}(a) - \boldsymbol{v}(a))[a(\boldsymbol{u}'(a) - \boldsymbol{v}'(a))]^{-1},\end{aligned} \tag{4.27}$$

where we have used the relationship given by equation (4.11) and the prime denotes the first-order derivative with respect to r. Since Ψ^{inc} is known, the evaluation of $\boldsymbol{v}(a)$ and $\boldsymbol{v}'(a)$ follows trivially. By including the R-matrix $\boldsymbol{R}^{\boldsymbol{u}}(a)$, which has been determined from the solution of the internal region, into equation (4.27) we obtain the matrix of solutions $\boldsymbol{x}(r)$ at $r = a$. These solutions are then propagated outward to the asymptotic radius $r = b$ using the same propagation routines as before. Equation (4.25) then yields the normalization vector $\boldsymbol{N}_m$ at $r = b$. Using equations (4.10), (4.16) and (4.25), it can be shown that the scattering amplitude $f_{lm}(\theta, \phi)$ is defined as

$$f_{lm}(\theta, \phi) = \sum_{l'} A_{l'mlm}N_{lm}Y_{l'm}(\theta, \phi), \tag{4.28}$$

where all the quantities on the right-hand side of (4.28) are known.

Downloaded from rsta.royalsocietypublishing.org

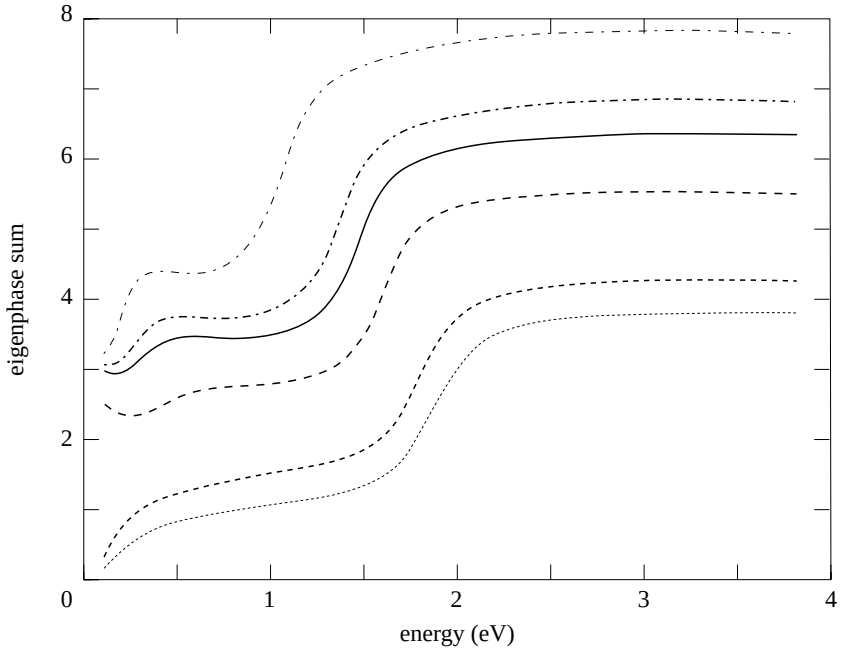

Figure 5. $^2\Sigma$ eigenphases; from top to bottom: $d = 5a_0, 7a_0, 8a_0, 10a_0, 15a_0$ and $20a_0$.

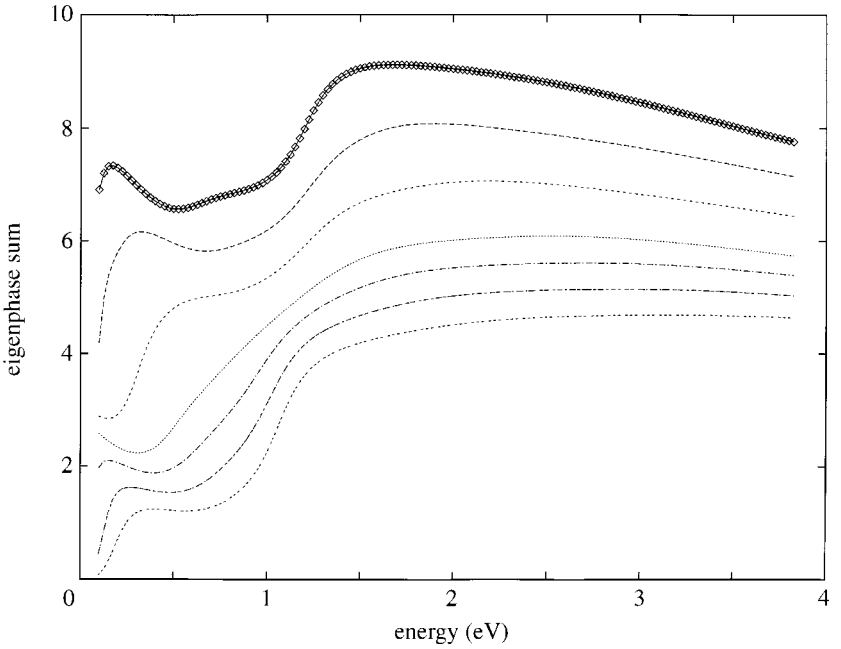

Figure 6. $^2\Sigma$ eigenphases; from top to bottom: $a = 17a_0, 16a_0, 15a_0, 14a_0, 13.5a_0, 13a_0$ and $12.5a_0$.

Downloaded from rsta.royalsocietypublishing.org

5. Results

In a preliminary calculation we considered the closed-shell molecule N_2 orientated perpendicularly on a metallic jellium surface. The surface was represented by equation (4.1), in which the value of the potential inside the surface was chosen to be 3.02 eV. We used the static exchange and polarization (SEP) approximation employed by Gillan *et al*. (1987) in which only the ground state ($^1\Sigma_g^+$) of N_2 was included in a Hartree–Fock representation. We also used the same two-particle–one-hole configurations in the second expansion of equation (4.4) in order that the target polarization was described accurately. This model gives very satisfactory results for low-energy electron scattering by gas-phase N_2 and in the case of $^2\Sigma_g$ scattering predicts a resonance position of *ca.* 2.4 eV which is in excellent agreement with experiment.

The effect of the surface was described in the internal region using expansion (4.2) in which we included all λ terms which gave non-zero coupling. In the present work, we required all terms up to and including $\lambda = 20$. We matched to a free-wave solution in the external region in order to obtain $^2\Sigma$ eigenphases in the energy range 0–4 eV. Although the results will be modified by the surface potential in the external region (this will be included in the next stage of the work), we are able to make some general comments on the main features of eigenphase sum behaviour.

Firstly, the perpendicular orientation of the adsorbed N_2 implies that the gerade/ungerade symmetry is broken but the projection of angular momentum m is conserved, i.e the eigenphases have $^2\Sigma$ symmetry. The results obtained by varying the adsorption distance d of the molecule from the surface are shown in figure 5. They indicate that for adsorption distances above $20a_0$, the molecule is sufficiently far from the surface that the position of the resonance in the eigenphase sum effectively coincides with the position of the $^2\Sigma_g$ resonance in scattering by gas-phase N_2. Furthermore, as the molecule is brought closer to the surface, the resonance is broadened and lowered in energy. This behaviour is similar to that observed in previous calculations by other workers. Figure 5 also shows evidence of resonances below 0.5 eV due to the temporary formation of what we refer to as surface states, i.e transient states in which the probe electron is trapped within the charge cloud of the adsorbate due to its own attraction to the surface. It is clear that when $d = 10a_0$ the lowest of these surface states has disappeared below threshold and become bound. The steady increase in the eigenphase sum just above threshold for $d < 10a_0$ is attributed to the formation of the next lowest surface state.

The eigenphases in figure 6 are produced by fixing the adsorption distance at $d = 5a_0$ and varying the radius a of the internal region. With increasing a, the position of the $^2\Sigma_g$ resonance is shifted slightly downward. As more of the surface is included, in increasingly larger internal region calculations, a series of surface states is formed below 0.5 eV with each state in turn becoming bound.

In future work this calculation will be extended to include nuclear motion in order to obtain vibrational cross-sections. We then intend to consider other molecules, including open-shell molecules orientated at an arbitrary angle to the surface, where several electronic states must be retained in the expansion. It is clear that the underlying surface atomic structure plays a significant role, especially for the most important cases of adsorption on transition and noble metal surfaces. This will demand going beyond the jellium substrate, to include strong atomic scattering where mul-

Downloaded from rsta.royalsocietypublishing.org

tiple scattering techniques may provide a suitable method. Our long-term aim is to be able to describe atomic scattering from surface adsorbates to sufficient accuracy that the interplay between theory and experiment will lead to a new understanding of adsorption.

We thank the EPSRC for their support in the funding of this project.

References

Aers, G. C. & Pendry, J. B. 1982 Calculation of the impact scattering contrbution to electron-energy loss spectra. *Comput. Phys. Commun.* **25**, 389–416.

Aers, G. C., Grimley, T. B., Pendry, J. B. & Sebastian, K. L. 1981 Electron-energy loss spectroscopy—calculation of the impact scattering from W(100)p(1 × 1)H. *J. Phys.* C **14**, 3995–4007.

Baluja, K. L., Burke, P. G. & Morgan, L. 1982 R-matrix propagation program for solving coupled second-order differential equations *Comput. Phys. Commun.* **27**, 299–307.

Bare, S. R., Hofmann, P., Surman, M. & King, D. A. 1983 Spatial intensity distributions from electron-impact scattering modes—W(100) (1 × 1)H. *J. Electron Spectr. Related Phenom.* **29**, 265–272.

Burke, P. G., Mackey, I. & Shimamura, I. 1977 *R-matrix theory of electron-molecule scattering* *J. Phys.* B **10**, 2497.

Davenport, J. W., Ho, W. & Schrieffer, J. R. 1978 Theory of vibrationally inelastic scattering from oriented molecules. *Phys. Rev.* B **17**, 3115–3127.

Demuth, J. E., Schmeisser, D. & Avouris, Ph. 1981 Resonance scattering of electrons from N_2, CO, O_2 and H_2 adsorbed on a silver surface. *Phys. Rev. Lett.* **47**, 1166–1169.

Djamo, V., Teillet-Billy, D. & Gauyacq, J. P. 1995 Low-energy electron scattering by N_2 molecules physisorbed on Ag: study of the resonant excitation process. *Phys. Rev.* B **51**, 5418–5428.

Duke, C. B. 1994 Interaction of electrons and positrons with solids: from bulk to surface in thirty years. *Surf. Sci.* **299/300**, 24–33.

Echenique, P. M. & Pendry, J. B. 1975 Absorption profiles at surfaces. *J. Phys.* C **8**, 2936–2942.

Eguiluz, A. G., Heinrichsmeier, M., Fleszar, A. & Hanke, W. 1992 First-principles evaluation of the surface barrier for a Kohn–Sham electron at a metal surface *Phys. Rev. Lett.* **68**, 1359–1362.

Gauyacq, J. P., Bahrim, B., Djabri, A., Djamo, V. & Teillet-Billy, D. 1997 In *Photon and electron collisions with atoms and molecules* (ed. P. G. Burke & C. J. Joachain), pp. 69–80. New York: Plenum.

Gerber, A. & Herzenberg, A. 1985 Resonance scattering of electrons from N_2 adsorbed on a metallic surface. *Phys. Rev.* B **31**, 6219–6227.

Gillan, C. J., Nagy, O., Burke, P. G., Morgan, L. A. & Noble, C. J. 1987 Electron scattering by nitrogen molecules. *J. Phys.* B **20**, 4585–4603.

Gonis, A. 1992 *Green functions for ordered and disordered systems.* Amsterdam: North-Holland.

Heinz, K., Saldin, D. K. & Pendry, J. B. 1985 Diffuse LEED and surface crystallography. *Phys. Rev. Lett.* **55**, 2312–2315.

Jennings, P. J. & Jones, R. O. 1986 Surface barrier in W(110). Low-energy electron-diffraction fine-structure analysis. *Phys. Rev.* B **34**, 6699–6703.

Jensen, E. T., Palmer, R. E. & Rous, P. J. 1990 Resonance electron scattering by O_2 monolayers on graphite. *Surf. Sci.* **237**, 153–172.

Jones, T. S., Ashton, M. R. & Richardson, N. V. 1989 An electron-energy loss study of the surface formate species chemisorbed on Ni(110)—dipole, impact and resonance scattering for adsorbed covered surfaces. *J. Chem. Phys.* **90**, 7564–7567.

Downloaded from rsta.royalsocietypublishing.org

Lang, N. D. & Kohn, W. 1970 Theory of metal surfaces: charge density and surface energy. *Phys. Rev.* B **1**, 4555–4568.

Palmer, R. E. & Rous, P. J. 1992 Resonances in electron scattering by molecules on surfaces. *Rev. Mod. Phys.* **64**, 383–440.

Pendry, J. B. 1994 Multiple scattering theory of electron diffraction. *Surf. Sci.* **299/300**, 375–390.

Pendry, J. B. & Saldin, D. K. 1984 SEXAFS without X-rays. *Surf. Sci.* **145**, 33–47.

Rous, P. J. 1995*a* Negative ion formation in adsorbed molecules: the role of surface states *Phys. Rev. Lett.* **74**, 1835–1838.

Rous, P. J. 1995*b* Surface crystallography: the experimental data base. In *Cohesion and structure of surfaces* (ed. F. R. de Boer & D. G. Pettifor), vol. 4, pp. 1–61. Amsterdam: Elsevier.

Rous, P. J., Palmer, R. E. & Willis, R. F. 1989 Resonance electron scattering from adsorbed molecules: angular distribution of inelastically scattered electrons and application to physisorbed O_2 on graphite. *Phys. Rev.* B **39**, 7552–7560.

Saldin, D. K. & Spence, J. C. H. 1994 On the mean inner potential in high-energy and low-energy electron difraction. *Ultramicroscopy* **55**, 397–406.

Saldin, D. K., Pendry, J. B., Van Hove, M. A. & Somorjai, G. A. 1985 Interpretation of diffuse low-energy electron-diffraction intensities. *Phys. Rev.* B **31**, 1216–1218.

Trioni, M. I., Brivio, G. P., Crampin, S. & Inglesfield, J. E. 1996 Embedding approach to the isolated adsorbate. *Phys. Rev.* B **53**, 8052–8064.

Van Hove, M. A. & Somorjai, G. A. 1994 Adsorption and adsorbate-induced restructuring: a LEED perspective. *Surf. Sci.* **299/300**, 487–501.

Van Hove, M. A., Weinberg, W. H. & Chan, C.-M. 1986 *Low-energy electron diffraction*. Berlin: Springer. *Ultramicroscopy* **55**, 397–406.

Wander, A., Held, G., Hwang, R. Q., Blackson, G. S., Xu, M. L., de Andres, P., Van Hove, M. A. & Somorjai, G. A. 1991 A diffuse LEED study of the adorption structure of disordered benzene on Pt(111) *Surf. Sci.* **249**, 21–34.

White, I. D., Godby, R. W., Rieger, M. M. & Needs, R. J. 1998 Dynamic image potential at an Al(111) surface. *Phys. Rev. Lett.* **80**, 4265–4268.

PHILOSOPHICAL TRANSACTIONS OF THE ROYAL SOCIETY A MATHEMATICAL, PHYSICAL & ENGINEERING SCIENCES

PHILOSOPHICAL TRANSACTIONS OF THE ROYAL SOCIETY A MATHEMATICAL, PHYSICAL & ENGINEERING SCIENCES